Author Manuscript
Faculty of Biology and Medicine Publication

This paper has been peer-reviewed but does not include the final publisher proof-corrections or journal pagination.

Published in final edited form as:

Title: Evidence for a TCR affinity threshold delimiting maximal CD8 T cell function.

Authors: Schmid DA, Irving MB, Posevitz V, Hebeisen M, Posevitz-Fejfar A, Sarria JC, Gomez-Eerland R, Thome M, Schumacher TN, Romero P, Speiser DE, Zoete V, Michielin O, Rufer N

Journal: Journal of immunology (Baltimore, Md. : 1950)
Year: 2010 May 1
Volume: 184
Issue: 9
Pages: 4936-46
DOI: 10.4049/jimmunol.1000173

In the absence of a copyright statement, users should assume that standard copyright protection applies, unless the article contains an explicit statement to the contrary. In case of doubt, contact the journal publisher to verify the copyright status of an article.

Unil
UNIL | Université de Lausanne
Faculté de biologie
et de médecine

Evidence for a TCR affinity threshold delimiting maximal CD8 T cell function

Daphné A. Schmid[1,*], Melita B. Irving[1,*], Vilmos Posevitz[2], Michael Hebeisen[3], Anita Posevitz-Fejfar[4], Floyd J-C. Sarria[5], Raquel Gomez-Eerland[6], Margot Thome[4], Ton N. M. Schumacher[6], Pedro Romero[2], Daniel E. Speiser[2], Vincent Zoete[7], Olivier Michielin[1,2,7,*] and Nathalie Rufer[1,2,3,*]

[1]Multidisciplinary Oncology Center (CePO), Lausanne University Hospital (CHUV), Lausanne, Switzerland

[2]Ludwig Institute for Cancer Research, Lausanne University Hospital (CHUV), Lausanne, Switzerland

[3]Department of Research, Lausanne University Hospital (CHUV), University of Lausanne, Lausanne, Switzerland

[4]Department of Biochemistry, University of Lausanne, Epalinges, Switzerland

[5]BioImaging and Optics platform, Faculty of Life Sciences, Ecole Polytechnique Fédérale de Lausanne (EPFL), Lausanne, Switzerland

[6]Department of Immunology, the Netherlands Cancer Institute (NKI), Amsterdam, the Netherlands

[7]Swiss Institute of Bioinformatics, Lausanne, Switzerland

[*] These authors contributed equally to this work

Address correspondence to:

Nathalie Rufer, PhD, Department of Research, CHUV/University of Lausanne, c/o Hôpital Orthopédique, niv 5, Aile Est, Avenue Pierre-Decker 4, CH-1011 Lausanne, Switzerland. Phone: +41 21 314 01 99. Fax: + 41 21 314 74 77. E-mail: Nathalie.Rufer@unil.ch

Olivier Michielin, MD, PhD, Swiss Institute of Bioinformatics, Quartier UNIL-Sorge, Bâtiment Génopode 2015, CH-1015 Lausanne, Switzerland. Phone: +41 21 692 40 53. E-mail: Olivier.Michielin@unil.ch

Running title: Affinity and avidity of NY-ESO-1 specific TCR variants

Word counts: 67’500 characters

Keywords: human, CD8 T cells, pMHC, T cell receptors, TCR gene transfer, lentiviral vectors, affinity, avidity, off-rates, TCR signaling, proliferation, cytolysis

Abbreviations: pMHC, peptide-MHC; WT, wild type

Grant Support: This study was sponsored and supported by the Swiss National Center of Competence in Research (NCCR) Molecular Oncology, the Ludwig Institute for Cancer Research, NY USA, the Swiss Institute of Bioinformatics, the NIH grant P41 RR-01081, the Swiss National Science Foundation grants 3200B0-118123 (N.R.), 3232B0-103172 and 3200B0-103173 (O.M.) and the Oncosuisse grant OCS-01995-02-2007 (N.R.). V.P. and P.R. were supported by the European Union FP6 Cancer Immunotherapy Grant. A.P.F. was supported by the Pierre Mercier Foundation.

Disclosures: The authors have no financial conflict of interests.

ABSTRACT

Protective adaptive immune responses rely on TCR-mediated recognition of antigen-derived peptides presented by self-MHC molecules. However, self-(tumor) antigen specific TCRs are often of too low affinity to achieve best functionality. To precisely assess the relationship between TCR-pMHC binding parameters and T cell function, we tested a panel of sequence-optimized HLA-A*0201/NY-ESO-$1_{157-165}$-specific TCR variants with affinities lying within physiological boundaries to preserve antigenic specificity and avoid cross-reactivity, as well as two outliers, i.e. a very high and a low affinity TCR. Primary human CD8 T cells transduced with these TCRs demonstrated robust correlations between binding measurements of TCR affinity and avidity, and the biological response of the T cells, such as TCR cell surface clustering, intracellular signaling, proliferation, and target cell lysis. Strikingly, above a defined TCR-pMHC affinity threshold ($K_D < \sim 5\ \mu M$), T cell function could not be further enhanced, revealing a plateau of maximal T cell function, compatible with the notion that multiple TCRs with slightly different affinities participate equally (co-dominantly) in immune responses. We propose that rational design of improved self-specific TCRs may not need to be optimized beyond a given affinity threshold, to achieve both optimal T cell function and avoidance of the unpredictable risk of cross-reactivity.

INTRODUCTION

Protective immune responses rely on the specific T-cell receptor (TCR)-dependent recognition of antigen-derived peptides bound to self-MHC molecules, and the strength of TCR-mediated antigen recognition is a major correlate of protection from disease (1-3). In melanoma patients, antigen-specific CD8+ T cell responses often develop, but their protective activity is limited. It has been shown that T lymphocytes directed against tumor antigens express TCRs of lower affinity/avidity for their antigenic ligands than pathogen-specific T cells (4). Apparently, mechanisms of self-tolerance shape self-antigen specific T cell repertoires with a relative lack of high affinity TCRs. Indeed, many of the tumor antigens recognized by cytotoxic T lymphocytes (CTL) are in fact self-antigens that are expressed by germ line cells and selected adult tissues, or by lineages of normal cells (5). Therefore, the relative lack of high affinity/avidity TCRs may be a major reason why immune responses towards self (tumor) antigens are often non-protective.

Unlike antibodies, TCRs do not undergo somatic hypermutation and affinity maturation, and peripheral T cells express TCRs of relatively weak affinity with K_D values in the range of 1-50 μM (6). This range may reflect on the one side the need to recognize foreign pMHC complexes with high specificity and maintain self-tolerance (7) and on the other side the need to efficiently elicit T cell activation. TCR “intrinsic affinity” is defined as the strength of binding of one TCR molecule to the pMHC complex. In contrast, TCR “binding avidity” defines, in the cellular context, the strength of binding between multiple TCRs to their respective pMHC complexes (reviewed in (8)). Because such assays integrate the potential effects of MHC coreceptors, TCR density and T cell activation state, it should not be confused with the measurements obtained for monomeric TCR affinities (8). Finally, the “functional avidity" represents the relative efficiency of T cell function based on antigen recognition via a defined TCR, and is assessed with stimulatory/target cells in presence of titrated peptide concentrations. Importantly, all aspects of TCR binding to pMHC (affinity, avidity and kinetic constants) have direct and/or indirect implications for T cell functional avidity. For instance, there is a close relationship between T cell functional avidity and target cell recognition as shown in several antigenic systems (2, 9-12) and collectively, results obtained from both mouse and human models suggest that T cells of high functional avidities are required for efficient anti-tumor immunity (reviewed in (5, 13, 14)). There is also a clear correlation between functional avidity of antigen recognition and the stability of pMHC multimer binding to TCR as measured by dissociation kinetic experiments, in which increased avidity correlated with slower TCR/multimer off-rates (15, 16).

Similar to the narrow window of TCR-Ag-binding affinities resulting from thymic selection and self tolerance mechanisms (7), various models have predicted that T cell activation may be limited to a window of affinities for the TCR-pMHC interaction and that above or below this window, T cells may not develop productive functions (8). In that context, selective loss of antigen-specific clonotypes that expressed low TCR-pMHC affinity has been observed, indicating that a minimum threshold of TCR binding must be achieved to clonally activate and select specific helper T cells (17). Studies based on cytokine secretion or killing assays using peptide loaded antigen-presenting cells as targets have shown that the minimum concentration of antigen required, to elicit a T cell response in terms of functional avidity was of ≈ 1 μM (18, 19). In contrast to these findings, several reports have recently examined T cells bearing engineered TCRs variants with affinities in the nanomolar range (20, 21) and found enhanced T cell function (22-26). However, when TCR affinity is enhanced to very high and supra-physiological affinities, T cells react with many different pMHC complexes and may lose defined antigen specificity, leading to dangerous cross-reactivity (24, 25, 27).

An important aspect often neglected from these studies is a detailed assessment of the impact of each optimized TCR variant on the TCR-pMHC binding avidity, down-stream signaling and functional avidity in engineered T lymphocytes. To specifically address this issue, we assessed a panel of affinity optimized TCR variants specific for the tumor antigen A*0201/NY-ESO-$1_{157\text{-}165}$ for pMHC binding and T cell function. These TCRs have been generated by a novel structure-based approach (28, 29) allowing the rational design of TCRs that preserve precise antigenic specificity and avoid cross-reactivity, unlike previously designed TCRs (20, 21). In the present study, we observed slower TCR-pMHC binding off-rates, increased TCR-pMHC multimerisation and intracellular signaling through p-LAT and p-ERK1/2 in T cells expressing high affinity TCR variants, supporting enhanced T cell functionality. Importantly, above a defined TCR affinity threshold, T cell avidity and function were not further enhanced, thus delimiting a plateau for maximal activity. Altogether, our data indicate that TCRs may not need to be optimized beyond a given affinity threshold to achieve best functionality.

MATERIALS AND METHODS

Cell lines and primary CD8 T lymphocytes

SUP-T1, melanoma cell lines (Me 275, Me 290 and NA8), T2-A2 (TAP-deficient lymphoblastoid cell line transfected with HLA-A*0201), C1R-WT and C1R-CD8null cells were cultured in RPMI 1640 (Invitrogen) supplemented with 10% fetal calf serum, 10 mM Hepes, penicillin (100 U/ml), and streptomycin (100 μg/ml). Peripheral blood mononuclear cells (PBMC) were obtained from two healthy donors by density centrifugation using Ficoll-Hypaque (Pharmacia Biotech). CD8 T lymphocytes were positively enriched using anti-CD8-coated magnetic microbeads (Miltenyi Biotec) and were either cryopreserved for later use or expanded after transduction in RPMI 1640 medium supplemented with 8% human serum, 150 U/ml recombinant human IL-2 (rhIL-2; a gift from GlaxoSmithKline), 1 μg/ml PHA (Remel, Lenexa, KS) and 1 x 10^6/ml irradiated (3000 rad) allogeneic PBMC as feeder cells. Culture medium was checked daily, changed when required and cells were stimulated every 20 days of culture.

Soluble TCR production and measurements of TCR affinity

The detailed procedure for the generation of high affinity TCR Vβ chains upon structure-based design is available elsewhere ((28, 29); Zoete and Michielin, *unpublished data*). Mutations were introduced into the WT TCR BV13.1 (patient LAU 155) DNA by PCR mutagenesis using the QuickChange mutagenenis kit (Strategene) and confirmed by DNA sequencing. In brief, TCR α (AV23.1) and TCR β (BV13.1) chains were subcloned by PCR separately into the pGMT7 bacteriophage expression vector and transformed into competent BL21(DE3)pLys cells. Proteins were purified from inclusion bodies, and the soluble alpha and beta TCR chains were refolded, concentrated, filtered and purified (via HIS-tag and SD200 columns) prior to SPR analysis. Binding kinetics for WT and variant TCRs, with biotinylated A2/NY-ESO-1 monomers was performed using the BIAcore 3000.

Generation of lentiviral constructs encoding WT and variant TCRs

The full length codon-optimized TCR AV23.1 and TCR BV13.1 (according to Arden's nomenclature (30)) chain sequences of a dominant T cell clone of patient LAU 155 (31) were cloned in the pRRL lentiviral transfer vector, a third generation HIV-based lentiviral vector, kindly provided by L. Naldini (32), in which most of the U3 region of the 3' LTR was deleted, resulting in a self-inactivating 3'-LTR or SIN. The most efficient LV construct consisted of the codon optimized TCR α-chain under the hPGK promoter, linked to the codon optimized TCR β-chain by an internal ribosomal entry site (IRES) and a kozac sequence to enhance translational efficiency (data not shown). Structure-based amino acid TCR substitutions were introduced into WT TCR sequence using the QuickChange MultiSite-Directed Mutagenesis Kit (Stratagene) and confirmed by DNA sequencing.

Lentiviral production and cell transduction

LV vectors were produced by transient transfection of 293T cells using a standard calcium phosphate precipitation protocol. In brief, 293T cells were co-transfected with the vector of interest (pRRL-hPGK-TCR Vα23.1-IRES-TCR Vβ13.1) and the lentiviral transfer vector, envelope and packaging plasmids (pRSV-Rev, pMD2-VSV-G, and pMDLg/pRRE). LV supernatants were harvested 24h and 48h after transfection, filtered and concentrated by ultracentrifugation. Pellets were resuspended in the appropriate volume of sterile cold PBS and either stored at -80°C or directly used. $1x10^6$/ml of SUP-T1 cells or $2x10^6$ /ml of CD8 T cells were transferred to pre-treated polybrene plates (1 μg/ml) and transduced with concentrated LV supernatant. Expression of transduced TCRs was measured by flow cytometry on d5 after transduction. LV production and cell transduction were conducted in at least three independent experiments and produced comparable results, indicating no major biases in the expression of the introduced TCRs.

Flow cytometry analysis

SUP-T1 and CD8 T cells expressing WT or variant NY-ESO-1-specific TCRs were stained with PE-labeled HLA-A2/NY-ESO-$1_{157-165}$ (SLLMWITQA) multimers as described previously (33) and/or with PE- or FITC-conjugated antibodies against BV13.1 (Beckman Coulter), CD4 or CD8 (Beckton Dickinson, San Diego, CA). Cross-reactivity of TCR variants was assessed as described above using PE-labeled A2/CMV (pp65, NLVPMVATV), A2/FluMA (GILGFVFTL), A2/MelanA$_{26-35}$ (ELAGIGILTV), A1/MAGE3 (EVDPIGHLY), and A3/FluMP (RLEDVFAGK) multimers. Flow cytometry analyses were performed on a LSR-II flow cytometer (BD Biosciences) and data were analyzed using CellQuest, FCS-Express or FlowJo software. Bulk CD8 T cells transduced with WT and variant TCRs were further enriched following sorting of multimer$^+$ T cells using a FACSVantage® SE machine (Becton Dickinson) and included CD8 T cells expressing the V49I TCR variant, despite the reduced proportion of multimer$^+$ stained cells. To allow direct comparison between the different transduced CD8 T cells, we used in every experiment, cell cultures that expressed similar levels of the TCR BV13 (ranging between 90 to 99%).

Multimer association and dissociation measurements

For association (on-rates) experiments, SUP-T1 expressing WT or variant NY-ESO-1-specific TCRs were first stained for 20 min at 4°C with FITC-labeled anti-CD4 mAb, washed once and resuspended in buffer. An aliquot (corresponding to time t_0) was taken and analyzed by flow cytometry. PE-labeled A2/NY-ESO-$1_{157\text{-}165}$ multimers (2 μg/ml) were then added to the samples and aliquots were collected at different time points and intensity of stainings was measured by flow cytometry. Transduced CD8 T cells were only stained with PE-labeled multimers. For dissociation experiments (off-rates), SUP-T1 and CD8 T cells transduced with WT or variant TCRs were first stained with PE-labeled A2/NY-ESO-$1_{157\text{-}165}$ multimers, followed for SUP-T1 cells by staining with FITC-labeled anti-CD4 mAb as described above. An aliquot (corresponding to time t_0) was taken and directly analyzed by flow cytometry. 5 μg/ml of OKT3 was added to the remaining samples to avoid rebinding of the multimers after dissociation from the TCR. MFI data were collected at different time points and expressed as the percentage of initial bound multimer that remained associated with the cells. $t_{1/2}$ for half maximal binding and k_{off} (min^{-1}) were determined.

Confocal microscopy analysis

TCR-transduced SUP-T1 cells were washed once in RPMI 1640 medium and pellets resuspended at $3x10^6$ density/ml. Staining was performed either with PE-labeled A2/NY-ESO-$1_{157\text{-}165}$ or A2/CMV$_{495\text{-}503}$ multimers at 4.4 µg/ml. 30 µl of cell suspension was pipetted per spot onto a 12 spot slide (Marienfeld) and incubated for 1 minute at 37^{o}C. To achieve proper attachment of the cells to the surface, the slides were placed for further 10 minutes to 4°C and remaining non-attached cells were washed away in PBS. The cells were fixed in 4% PFA. Following 3 washing steps, nuclei were stained with Hoechst 33342. Samples were embedded in mounting media (Dabco™) and a cover slip was fixed to the slide with nail polish. Images were acquired using scanning confocal microscope (LEICA SP2 AOBS, 63x/1.4x Apocromat objective, LEICA-Microsystems, Germany) and using LCS 2 acquisition software. Raw images were deconvolved using HuygensPRO software (Scientific Volume Imaging, Holland) to gain image quality and then Metamorph software (Molecular Devices, USA) was used for segmentation and analysis. First, a journal has been made to count automatically the number of cells based on standard area of the nuclei stained with Hoechst 33342. Then, after a manual selection around cell membrane (interactive pen display, Cintiq 21UX, WACOM), a second journal measured the surface of the cell and cut its border by an erosion of 2 micron allowing the quantification of surface (high intensity clusters) and total fluorescence of the cell membrane fluorescence.

Western blot analysis

Typically $2x10^6$ CD8 T cells per lane or $1x10^6$ SUP-T1 cells per lane were used for biochemical analysis. For all experiments, transduced CD8 T cells or SUP-T1 cells were either left unstimulated or stimulated with OKT3 (10 µg/ml) for 10 min or with A2/NY-ESO-$1_{57\text{-}165}$ multimer (10 µg/ml) at indicated time-points, at 37C° in RPMI. All stimulations were performed in the presence of 10 µg/ml of anti-CD28 antibody (BD Biosciences). Cells extracts were obtained by resuspending the pellets in lysis buffer containing 1% Nonidet P-40, 1% lauryl maltoside (n-dodecyl-beta-D-maltoside), 50 mM Tris (pH 7.5), 140 mM NaCl, 10 mM EDTA, 10 mM NaF, 1 mM phenyl-methylsulfonylfluorid, and 1 mM Na_3VO_4. Post-nuclear supernatants were subjected to immunoblotting. Proteins were separated by SDS-PAGE followed by electrotransfer to nitrocellulose membranes. Subsequently, membranes were probed with the following Abs: anti-phospho-tyrosine 4G10 (Upstate/Millipore), anti-phospho-LAT Y-171 and anti-phospho-ERK1/2 (Cell Signaling Technology). Membranes were stripped in buffer containing 0.7 % 2-β-Mercaptoethanol, 2 % SDS, and 0.06M TRIS pH 6.7 at 56°C for 25 min, then washed and re-probed with anti-β-actin mouse Ab (Sigma, Clone AC-15).

CFSE proliferation and chromium release assays

CFSE-labeled CD8 T cells ($0.5x10^6$) transduced with WT or variants TCRs were incubated with T2 target cells ($0.5x10^5$) pulsed with analog NY-ESO-$1_{157\text{-}165}$ peptide (0.01 μg/ml, SLLMWITQA) or CMV pp65 peptide (1 μg/ml, NLVPMVQTV) in RPMI supplemented with 8% human serum. 10 U/ml IL-2 was added 48h after stimulation. On day 3 and 4, $2x10^5$ cells were collected and analyzed on a LSRII flow cytometer. The percentage of CD8 T cells proliferating (CFSE^{low}) in response to NY-ESO-1-specific stimulation was estimated from the proportion of corresponding CFSE-labeled cells (CFSE^{high}) stimulated with the irrelevant CMV peptide.

Lytic activity and antigen recognition was assessed functionally in 4h ^{51}Cr-release assays using (i) T2 target cells or C1R target cells that expressed either wild-type or CD8-null HLA-A2 (HLA-A2$^+$/TAP$^{-/-}$) pulsed with serial dilutions of analog NY-ESO-$1_{157\text{-}165}$ peptide (SLLMWITQA (34)), or Melan-$A_{26\text{-}35\ A27L}$ peptide (ELAGIGILTV) as well as using (ii) the melanoma cell lines Me 275 (A2$^+$/NY-ESO-1$^+$), Me 290 (A2$^+$/NY-ESO-1$^+$), and NA8 (A2$^+$/NY-ESO-1$^-$) incubated in the presence or absence of the analog NY-ESO-$1_{157\text{-}165}$ peptide. The percentage of specific lysis was calculated as 100 x ((experimental - spontaneous release)/(total - spontaneous release)).

Statistics

The results were analyzed by unpaired two-sample *t* test, one-phase exponential decay and log-log linear regression analyses, and log sigmoid curve fitting using GraphPad Prism version 5.02 (GraphPad Software).

RESULTS

Selection of a panel of reengineered NY-ESO-1-specific TCR variants with progressive increased affinities

Recently, we identified dominant T cell clonotypes from melanoma patient LAU 155 who mounted a strong natural immune response against the cancer testis antigenic epitope HLA-A*0201/NY-ESO-$1_{157\text{-}165}$ (31, 35). One of them expressed the TCR AV23-BV13 (named BV13-clono1) that is closely related to the 1G4 TCR for which a crystal structure (2BNR in the Protein Databank) has been reported (36). The sequence of 1G4 differs from BV13-clono1 by only four amino acid residues, two within the CDR3α loop (T95Q and S96T) and two within the CDR3β loop (N97A and T98A). This experimental structure (2BNR) allowed the application of a novel *in silico* structure-based TCR approach to rationally design sequence mutations of the BV13-clono1 TCR ((28, 29); Zoete V, Irving M, Ferber M, Schmid D, Rufer N, and Michielin O. *manuscript in preparation*). Based on these *in silico* calculations, five NY-ESO-1 specific TCR variants were selected for this study, with amino acid replacements in the CDR2β (V49, G50, A51) and CDR3β (A97) (Table I). Residues V49, G50 and A51 mostly interact with the HLA-A*0201 molecule, whereas A97 primarily binds to the NY-ESO-1 peptide. We characterized the affinity (Table I) of these mutants and of an additional triple TCR variant that combines G50A, A51E (CDR2β) and A97L (CDR3β) substitutions for the pMHC complex by Surface Plasmon Resonance (SPR). When compared to the WT TCR (K_D, 21.4 μM), TCRs variants showed an incremental hierarchy in affinity from single mutants (A51E < G50A < A97L) to the double mutant G50A+A51E (K_D, 1.9 μM), and to the triple mutant G50A+A51E+A97L (K_D, 0.9 μM, 23-fold increase). We did not assess the

V49I TCR variant, since it displayed very poor binding to pMHC when titrated by ELISA (data not shown).

Cell surface binding avidity of NY-ESO-1 specific TCR variants strongly correlating with their respective soluble TCR-pMHC affinity

All TCR variants specific for NY-ESO-1/A2 were transduced in SUP-T1 cells (37) and primary bulk CD8+ T cells using the VSV-G pseudotype third generation of lentiviral (LV) vectors. We also included the closely related 1G4 TCR (36), and an adapted wtc51 TCR previously selected upon bacteriophage library screening for its nanomolar range of affinity towards the A2/NY-ESO-1 complex (21) (Table I). Together with WT (BV13-clono1) and 1G4 TCRs, these TCR variants represent a selection of NY-ESO-1-specific TCRs that can be classified according to an incremental hierarchy of monomeric soluble TCR-pMHC affinities (Table I). We sought to determine whether a progressive increase in multivalent TCR-pMHC binding avidities would similarly be observed when assessed at the surface level of T lymphocytes. To address this issue, we first measured the percentage of specific multimer binding by SUP-T1 (supplemental Fig. 1A) and bulk CD8 T (Fig. 1A) cells transduced with the different TCR variants. All transduced cells expressed comparable levels of TCR Vβ13 as assessed by staining with an anti-BV13 mAb. With the exception of the V49I TCR mutant, the proportion of multimer-positive T cells was comparable, ranging between 88 and 99%. This result indicates that V49I TCR mutant likely forms TCR-pMHC complexes of relative low stability at the surface of T lymphocytes, in accordance to the finding that the soluble version of this TCR poorly binds the pMHC (data not shown). Moreover, we also observed that none of the transduced T cells had significant binding for (i) pMHC presenting irrelevant peptide epitopes (i.e. CMV, Flu, Melan-A) or (ii) allogeneic HLA-A1 or-A3 multimers (Fig. 1A, data not shown).

We then assessed cell surface bound multimer on-rates (supplemental Fig. 1B and Fig. 1B) and off-rates (supplemental Fig. 1C and Fig. 1C). Analysis of multimer association rates revealed a rapid initial increase of the mean fluorescence intensity (MFI) for all transduced cells, either within the first hour (SUP-T1 cells) or first 20 min (CD8 T cells), accompanied of substantial MFI differences between the TCR variants after 120 min. Indeed, V49I TCR mutant always showed the lowest mean fluorescence at equilibrium, whereas G50A, A97L, G50A+A51E, and G50A+A51E+A97L mutants systematically had higher MFI than the WT TCR. Importantly, the dissociation kinetics varied between the TCR variants and could be classified into the following hierarchy: V49I < WT = 1G4 < A51E < A97L < G50A = G50A+A51E < G50A+A51E+A97L < wtc51 (supplemental Fig. 1C and Fig. 1C). Comparable rates of association and dissociation were observed between WT (BV13-clono1) and 1G4 TCRs, that represent the two natural unmodified TCRs. Remarkably, the dissociation rate constant (k_{off}, min^{-1}) of the pMHC from the TCR variants in transduced T cells (supplemental Fig. 1D and Fig. 1D) showed excellent correlation with the monomeric TCR-pMHC affinities (K_D) as well as with dissociation rates (k_{off}, s^{-1}) measured by SPR (supplemental Fig. 1E and Fig. 1E). Collectively, these results support the notion that TCR multimer off-rates directly and strongly correlate with monomeric TCR-pMHC affinities, being faster for TCRs of relatively low affinity (e.g. V49I, WT, 1G4, and A51E) and slower for TCRs of higher affinities (e.g. A97L, G50A, G50+A51E and G50A+A51E+A97L). In line with these results, both SUP-T1 cells and CD8 T cells expressing the modified wtc51 TCR variant of nanomolar range affinity exhibited the slowest multimer off-rates (with an average mean $t_{1/2}$ of 62 min for CD8 cells). Of note, the natural T cell clone (TCC) from which the WT TCR BV13-clono1 had been originally isolated (31) depicted slower off-rates when compared to CD8 T cells transduced with the same WT TCR (Fig. 1). This effect may best be explained by the higher level of expressed TCRs (increased MFI) by the original clone that could impact on both the association and dissociation rates through increased pMHC binding avidity (8).

Enhanced multivalent clustering of a TCR variant with increased affinity in cell membranes of SUP-T1 cells

We next examined fluorescence intensity and clustering of TCR-pMHC complexes in transduced SUP-T1 cells at the single cell level using scanning confocal microscopy, deconvolution and image processing (Fig. 2). In accordance with the TCR-pMHC affinity and binding avidity data, SUP-T1 cells transduced with the G50A+A51E TCR variant exhibited increased clustering of TCR-pMHC complexes in individual cells, when compared to SUP-T1 cells expressing WT or V49I TCRs. Moreover, we observed statistically significantly stronger fluorescence intensity signals in the cytoplasm, suggesting enhanced internalization of the TCR-pMHC complex in those cells (Fig. 2). In contrast, both relative intensity fluorescence and frequency of high intensity clusters per cell were strikingly reduced for the V49I TCR mutant, in line with the observation that this particular TCR possesses poor binding avidity for the A2/NY-ESO-1 complex.

Higher levels of LAT and ERK phosphorylation and increased proliferation in CD8 T cells transduced with a high affinity TCR variant

Several studies have shown that multivalent clustering of TCRs is necessary for T cell signaling and activation (38, 39). Therefore, we examined whether the increase in TCR-pMHC clustering observed in SUP-T1 cells expressing G50A+A51E TCR mutant (Fig. 2), would also lead to an enhanced activation of downstream TCR signaling proteins such as LAT (Linker for Activation of T cells) and ERK (Extracellular signal-Regulated Kinase) 1/2. Following multimer stimulation, Western blot analysis revealed a drastic reduction of ERK phosphorylation levels in both SUP-T1 and CD8 T cells expressing the V49I TCR mutant, highly contrasting with phospho-ERK levels found in WT and G50A+A51E transduced T cells (Fig. 3A). Importantly, there were no differences in phosphorylation upon stimulation of the cells with the anti-TCR Ab OKT3, indicating that the TCR-mediated signaling machinery leading to MAPK activation was fully functional. A kinetic analysis revealed that LAT phosphorylation was rapid and transient, with maximal phosphorylation of residue Y171 being reached after only one minute following specific stimulation (Fig. 3B and 3C). Strikingly, LAT phosphorylation was higher in primary CD8 T cells transduced with the G50A+A51E mutant than in cells expressing WT TCR. Also, increased basal levels of phosphorylation were already detectable in G50A+A51E transduced CD8 T cells in the absence of multimer stimulation (Fig. 3C, see insert). Finally, more rapid and sustained ERK2 phosphorylation was observed in G50A+A51E transduced CD8 T cells, reaching up to a 7-fold increase when compared to cells expressing WT TCR (Fig. 3C).

Activation of ERK has been shown to be essential in mediating T cell function such as proliferation (40, 41). Therefore, we conducted a quantitative cytometric analysis of the proliferative response of T cells to T2 cells loaded with the NY-ESO-$1_{157-165}$ peptide, using CFSE as an indicator of cell division (Fig. 3D). In agreement with the stronger and more sustained MAPK activation, CD8 T cells transduced with the G50A+A51E mutant showed an increased proliferative capacity as compared to cells transduced with WT TCR. Conversely, reduced proliferation potential was found for T cells expressing V49I, correlating with the low levels of phospho-ERK expression in those cells. Finally, no differences in relative proliferation were observed for T cells expressing A51E, A97L and G50A+A51E+A97L, consistent with the observation that levels of p-LAT and p-ERK1/2 for the A97L TCR variant, tested in addition, were not higher than for the WT TCR (data not shown).

TCR variants of increased affinity reveal enhanced T cell functionality but reach a plateau of maximal activity

In order to evaluate functional avidity and fine specificity of antigen recognition by our panel of transduced CD8 T cells, we conducted chromium release assays to assess their ability to recognize target cells pulsed with graded concentrations of NY-ESO-$1_{157-165}$ peptide (Fig. 4A). All transduced CD8 cells were able to recognize and lyse T2 target cells loaded with the cognate peptide but not with irrelevant peptides (i.e. FluMA, CMV pp65 or Melan-A/MART-1; data not shown). T cells transduced with V49I TCR required about 100-fold more peptide than WT TCR-transduced CD8 T cells to achieve comparable and efficient lysis (Fig. 4A and Fig. 4B). The remaining transduced CD8 T cells fell into two distinct groups. Those in the first group, including WT, A51E and 1G4 TCR variants, shared similar functional avidity, as they required similar peptide concentrations to achieve half-maximal lysis of T2 cells. The second group comprised mostly cells expressing TCR variants of increased binding affinity/avidity to pMHC, namely G50A, G50A+A51E, A97L, and G50A+A51E+A97L, and demonstrated statistically significant superior functional avidity over WT cells (median of 50% maximal target cell lysis, 0.04 nM versus 0.18 nM). Remarkably, the concentrations of NY-ESO-$1_{157-165}$ peptide that yielded half-maximal activity were highly similar for the different members of this group, and correlated to the activity observed for the natural T cell clone (TCC, data not shown).

Altogether our results reveal a robust correlation between multimeric TCR-pMHC binding off-rates (k_{off}, min^{-1}) and functional killing activity; there was a drastic reduction in killing function of T cells expressing the lowest binding avidity TCR (e.g. V49I), and conversely, enhanced function in those cells of highest TCR binding avidities (Fig. 5A). Our results also show a nice correlation between T cell functional avidity and monomeric TCR-pMHC affinity. Importantly, above a given TCR affinity threshold (delineated by the affinity of the A51E TCR variant, $K_D < 7.1\ \mu M$), T cell function could not be further enhanced as demonstrated by the comparable functional avidities obtained for the second group of transduced T cells (Fig. 5A, circles). Finally, bulk CD8 T cells that stably expressed the wtc51 TCR variant of nanomolar affinity showed an unexpected reduced functional avidity when compared to WT cells (EC50, 0.86 ± 0.3 nM versus 0.18 ± 0.1 nM, respectively; Fig. 4).

CD8 T cells expressing TCRs of increased affinity exhibit lower CD8 dependency

To analyze CD8 dependency of target cell recognition by CD8 T cells expressing TCRs of progressive affinities, C1R cells transfected with mutant HLA-A2 molecules that abrogate CD8 binding (42) were used as target cells (Fig. 5B). WT TCR and variants A51E and A97L exhibited inferior functional avidity of antigen recognition compared to cells expressing variants G50A+A51E and G50A+A51E+A97L. In contrast, T cells expressing the low avidity receptor V49I did not recognize C1R CD8 null target cells at any concentration of NY-ESO-$1_{157\text{-}165}$ peptide tested. These data indicate that T cells bearing TCRs with higher binding strength ($K_D \leq 1.9$ μM) are less dependent for CD8-MHC interactions than ones expressing TCRs of weaker affinities.

Specific and enhanced tumor cell recognition by CD8 T cells expressing TCR variants of increased affinity

Finally, we investigated the capacity of CD8 T cells transduced with TCRs of varying affinities to specifically recognize and lyse tumors expressing the naturally processed NY-ESO-1 epitope (Fig. 6). Except for V49I, all of the transduced T lymphocytes efficiently killed the Me 275 and Me 290 melanoma tumor cell lines (Fig. 6A). The relative tumor killing activity of transduced T cell variants was estimated as the ratio of the percentage of specific lysis obtained without adding exogenous NY-ESO-$1_{157\text{-}165}$ peptide (Fig. 6A) versus that obtained after adding exogenous peptide (Fig. 6B). T cells transduced with V49I variant exhibited a ratio close to 0, indicating that such cells were unable to recognize tumor cells when no exogenous peptide was added (Fig. 6C). In contrast, WT cells with ratios around 0.5 showed intermediate tumor cell recognition and lysis. Remarkably, tumor reactivity was progressively enhanced up to ratios of close to 1 for T cells expressing TCR variants of higher affinity, corresponding with their incremental affinity hierarchy. These results demonstrate that such T cell variants have the ability to strongly recognize NY-ESO-1 naturally expressing tumor cells (Fig. 6A and 6C). However, this effect became abrogated for the two TCR variants of highest affinity (G50A+A51E+A97L, wtc51), and this was particularly evident for the tumor reactivity observed against Me 275 cell line (Fig.

6C). The finding that NY-ESO-1 negative NA8 cell line (HLA-A*0201$^+$) was not killed by the majority of transduced CD8 T cells, indicates that cross reactivity with other naturally processed tumor peptides expressed by this cell line is likely to be excluded (Fig. 6C).

DISCUSSION

Adoptive transfer of TCR-gene modified T cells has been recently developed with the aim to induce immune reactivity toward defined tumor-associated antigens to which the endogenous T cell repertoire is non-responsive (reviewed in (43, 44)). The feasibility of TCR gene transfer was initially demonstrated in a phase I clinical trial whereby melanoma patients received autologous peripheral blood lymphocytes (PBLs) transduced with a specific TCR against the differentiation antigen Melan-A/MART-1 (45). More recently, Johnson and colleagues conducted another extensive study in patients with metastatic melanoma (46) treated with genetically engineered T lymphocytes, and demonstrated persistence in the blood of the transduced cells as well as objective cancer regressions. However, patients exhibited in addition toxicity with destruction of normal melanocytes in the skin, eye and ear, indicating that T cells expressing highly reactive Melan-A specific TCRs also targeted normal tissues expressing the cognate antigen (46). These results underline not only the cytotoxic potency in vivo, but also the importance of the tissue distribution of tumor (self) antigen expression. Therefore, much attention has been focused on the choice of antigen specificity (47). The cancer testis antigen NY-ESO-1 appears to be a preferred choice, since its expression is found in melanoma and many other types of cancer cells but not in somatic adult tissues, with the exception of testis cells that do not express MHC molecules.

One highly promising approach towards the improvement of adoptive cell transfer cancer therapy utilizing TCR gene transfer is to modify TCR sequences in order to increase their affinity for cognate tumor antigen epitopes (43, 44). Recently, various strategies, such as phage-display TCR library screenings, have led to the generation of 1G4 TCR variants with supra-physiological binding strength for the NY-ESO-1_{157-}

$_{165}$ epitope of up to picomolar affinities (20, 21). Although some of the variants identified showed enhanced T cell function, the increase in affinity oftentimes also led to loss of target cell specificity (24). Interestingly, Robbins and colleagues recently defined an upper affinity limit for these 1G4 TCR mutants in CD8 T cells that is compatible with specific antigen recognition and lies between 450 and 280 nM (25). At present, the major challenge is no longer to simply maximize the affinity of any given self tumor-reactive TCRs but to finely tune and optimize TCR affinity and binding kinetics in a step-by-step approach to maximize T cell functionality. This implies to precisely determine the impact of each optimized TCR variant on its binding to pMHC, downstream signaling and subsequent T cell function.

In this study, we characterized a selected panel of TCR variants specific for the peptide-MHC ligand A2/NY-ESO-1$_{157-165}$ and derived from the original TCR BV13-clono1 (31). These TCR variants were designed by a novel structural-based modeling approach allowing the step-by-step increase of the affinity to the TCR in a highly controlled manner ((28, 29); Zoete V, Irving M, Ferber M, Schmid D, Rufer N, and Michielin O. *manuscript in preparation*). The latter relies on (i) the identification of individual amino acid residues of defined importance for the TCR/pMHC interaction and binding, (ii) structure-based design of corresponding putative sequence modifications and (iii) their selection based on the calculated binding free energy change upon mutation. Affinities of the predicted TCRs followed an incremental hierarchy, from 21.4 μM (WT) up to 0.91 μM (G50A+A51E+A97L), lying within physiological boundaries (6), and below the affinity threshold described for antigen cross-reactivity (25). We also included two outliers. The first one comprised the V49I TCR variant, the only TCR predicted to have an unfavorable $\Delta\Delta G_{bind}$ value, and for which titration ELISA revealed extremely low levels of binding to pMHC (data not shown). The second outlier assessed, the TCR wtc51, was adapted from Dunn et al. (21), and had the highest affinity of all TCRs characterized (K_D = 15 nM).

A major finding of this study is the remarkable correlation between monomeric soluble TCR-pMHC binding affinity (K_D) and multimeric TCR-pMHC dissociation kinetics on T cells ($t_{1/2}$), with faster off-rates for TCRs of relatively low affinity as compared to TCRs of increased affinity (supplemental Fig. 1 and Fig. 1). This was particularly evident for the V49I and wtc51-modified TCR variants showing the fastest and slowest dissociation rates, respectively. Strong correlations were not only found with transduced SUPT1 cells expressing relatively low levels of the CD8 coreceptor, but also with primary CD8 T cells. Collectively, elevated TCR affinities resulted into the slower dissociation rates of pMHC multimers from the surface of T cells expressing those receptors. Yet it still remains unclear whether an increase in the $t_{1/2}$ of the binding of the TCR to the A2/NY-ESO-1 complex would translate into a greater clustering and multimerization process. Here, we demonstrate that T cells transduced with the TCR variant (G50A+A51E), of increased affinity and relatively slow off-rate, underwent enhanced TCR aggregation and clustering upon engagement with multimers, which may account for the markedly enhanced LAT and ERK1/2 phosphorylation and proliferation of those cells (Fig. 2 and 3). In sharp contrast, the cells transduced with the V49I variant, having the lowest binding capacity for pMHC, displayed less frequent multimerization per cell, barely detectable levels of phospho-ERK, and limited proliferation and tumor killing. This is to our knowledge, the first time that the impact of single or dual TCR amino acid replacement has been comprehensively assessed, and directly translated into positive (e.g. G50A+A51E) or negative (e.g. V49I) changes in TCR-pMHC binding parameters (such as affinity, avidity, and clustering), down-stream signaling pathways, and cellular functionality (T cell proliferation and target cell killing).

Major efforts have been made to characterize and identify specific binding parameters (K_D or half-life) that control T cell activation (reviewed in (8, 48)). Kinetic models of TCR-ligand interaction propose that functional potency is primarily determined by the duration of the TCR-pMHC interaction (49, 50), because sufficiently long dissociation rates may be required for completion of intracellular signaling cascades and subsequent T cell activation. The serial triggering hypothesis (51) whereas, suggests that dissociation rates need to be sufficiently short to allow an optimal dwell-time of interaction between the TCR and the pMHC complex so that multiple TCRs on the cell surface can sample the pMHC complexe for efficient T cell activation (52). These models are not mutually exclusive, and indeed our results are consistent with both of them. First of all, we observed that TCR/multimer off-rates directly correlated with functional avidity (as determined by the peptide concentration require to achieve half-maximal target lysis). Thus, slower dissociation rates were found for the transduced CD8 T cells of relatively high functional avidity (e.g. G50A, A97L, and G50A+A51E), in stark contrast with T cells expressing TCR variants of faster off-rates (e.g. V49I and WT), which displayed poor or less efficient functional avidity (Fig. 5). Secondly, TCRs variants of slowest dissociation rates (e.g. G50A+A51E+A97L, and wtc51-modified) showed reduced killing of cognate tumor cell lines (Fig. 6), suggesting that these prolonged k_{off} constant rates may lie outside the optimal range for efficient T cell functionality (i.e. serial triggering may be limiting). Indeed, this rather surprising observation was particularly evident for the wtc51 TCR variant (K_D of 15 nM), which displayed both limited functional avidity (as measured by EC50) and tumor killing activity. Increased TCR affinity, up to the nanomolar range, has mostly been associated with the loss of target cell specificity (24, 25). Our data now indicate that increases in T cell reactivity may also be accompanied by a significant reduction in the specific anti-tumor T cell response (Fig. 6D).

Recently, Chervin and coworkers (53) investigated the specific role of CD8 coreceptor on a large panel of 2C TCR affinity variants specific for SIYR/K^b. In their study, they measured the IL-2 release by transduced CD8 coreceptor-negative T cell hybridomas, and found a relatively sharp affinity cut-off between full activity or no activity, which likely defines the CD8 requirement threshold. Indeed, CD8 molecules likely play an important role by both stabilizing the binding the TCR to pMHC complexes, and by enhancing intracellular signaling and lowering the threshold of T cell activation (reviewed in (8)). Strikingly, our data also point to the existence of a TCR affinity threshold but for maximal T cell anti-tumor response. Indeed, those T cells whose TCRs had an affinity above a given threshold showed enhanced killing avidity when compared to WT T cells, but only up to a maximal activity plateau (equivalent to an average EC_{50} peptide concentration of 0.04 nM) (Fig. 4). Not surprisingly, with increased TCR affinities, the T cells became less CD8 dependent (Fig. 5)(42). Altogether, our data provide new evidence that the CD8 T cell function is controlled within a given window of TCR-pMHC-binding affinities. On the one hand, minimal TCR affinity is needed for T cell activation, also defined as the agonist threshold, and nicely illustrated in this study by the V49I TCR variant (see model, Fig. 6). On the other hand, T cells are also defined by a plateau of maximal activity revealing a TCR affinity threshold (depicted in our model by K_D < A51E TCR variant). Overall, these data indicate that there is no need to optimize TCRs for pMHC binding above a certain affinity threshold, because this may not lead to further enhanced activity.

The native WT TCR BV13-clono1 isolated from patient LAU 155 itself already shows very good affinity/avidity, and induces a functional activity closely related to the plateau of optimal T cell function (Fig. 6D). Since this TCR is highly representative for a large number of co-dominant NY-ESO-1 specific TCRs (31), it also indicates that optimized TCRs with this specificity are very likely to confer enhanced elimination of NY-ESO-1 positive tumors. The findings described here highlight the importance and feasibility of generating anti-tumor specific TCRs of optimal function (e.g. G50A, A97L, and G50A+A51E). Such studies are essential to understand and further promote therapeutic immune interventions like vaccination and adoptive T cell-therapy.

ACKNOWLEDGEMENTS

We are thankful to Drs I. Luescher and P. Guillaume for synthesis of multimers, and to M. André, P. Baumgaertner, M. Bruyninx, D. Hacker, N. Montandon, M. van Overloop, P. Reichenbach and S. Wieckowski for excellent technical and/or secretarial help, and helpful discussions. We also thank the VITAL-IT project of the Swiss Institute of Bioinformatics (Lausanne, Switzerland) for providing the computational resources.

REFERENCES

1. Speiser, D. E., D. Kyburz, U. Stubi, H. Hengartner, and R. M. Zinkernagel. 1992. Discrepancy between in vitro measurable and in vivo virus neutralizing cytotoxic T cell reactivities. Low T cell receptor specificity and avidity sufficient for in vitro proliferation or cytotoxicity to peptide-coated target cells but not for in vivo protection. *J. Immunol.* 149:972-980.
2. Alexander-Miller, M. A., G. R. Leggatt, and J. A. Berzofsky. 1996. Selective expansion of high- or low-avidity cytotoxic T lymphocytes and efficacy for adoptive immunotherapy. *Proc. Natl. Acad. Sci. USA* 93:4102-4107.
3. Gallimore, A., T. Dumrese, H. Hengartner, R. M. Zinkernagel, and H. G. Rammensee. 1998. Protective immunity does not correlate with the hierarchy of virus-specific cytotoxic T cell responses to naturally processed peptides. *J. Exp. Med.* 187:1647-1657.
4. Dunn, G. P., L. J. Old, and R. D. Schreiber. 2004. The three Es of cancer immunoediting. *Annu. Rev. Immunol.* 22:329-360.
5. Boon, T., P. G. Coulie, B. J. Van den Eynde, and P. van der Bruggen. 2006. Human T cell responses against melanoma. *Annu. Rev. Immunol.* 24:175-208.
6. Davis, M. M., J. J. Boniface, Z. Reich, D. Lyons, J. Hampl, B. Arden, and Y. Chien. 1998. Ligand recognition by alpha beta T cell receptors. *Annu. Rev. Immunol.* 16:523-544.
7. Savage, P. A., and M. M. Davis. 2001. A kinetic window constricts the T cell receptor repertoire in the thymus. *Immunity* 14:243-252.
8. Stone, J. D., A. S. Chervin, and D. M. Kranz. 2009. T-cell receptor binding affinities and kinetics: impact on T-cell activity and specificity. *Immunology* 126:165-176.

9. Yee, C., P. A. Savage, P. P. Lee, M. M. Davis, and P. D. Greenberg. 1999. Isolation of high avidity melanoma-reactive CTL from heterogeneous populations using peptide-MHC tetramers. *J. Immunol.* 162:2227-2234.

10. Zeh, H. J., 3rd, D. Perry-Lalley, M. E. Dudley, S. A. Rosenberg, and J. C. Yang. 1999. High avidity CTLs for two self-antigens demonstrate superior in vitro and in vivo antitumor efficacy. *J. Immunol.* 162:989-994.

11. Dudley, M. E., M. I. Nishimura, A. K. Holt, and S. A. Rosenberg. 1999. Antitumor immunization with a minimal peptide epitope (G9-209-2M) leads to a functionally heterogeneous CTL response. *J. Immunother.* 22:288-298.

12. Dutoit, V., V. Rubio-Godoy, P. Y. Dietrich, A. L. Quiqueres, V. Schnuriger, D. Rimoldi, D. Lienard, D. Speiser, P. Guillaume, P. Batard, J. C. Cerottini, P. Romero, and D. Valmori. 2001. Heterogeneous T-cell response to MAGE-A10(254-262): high avidity-specific cytolytic T lymphocytes show superior antitumor activity. *Cancer Res.* 61:5850-5856.

13. Gilboa, E. 1999. The makings of a tumor rejection antigen. *Immunity* 11:263-270.

14. Rosenberg, S. A., M. E. Dudley, and N. P. Restifo. 2008. Cancer immunotherapy. *N. Engl. J. Med.* 359:1072.

15. Dutoit, V., V. Rubio-Godoy, M. A. Doucey, P. Batard, D. Lienard, D. Rimoldi, D. Speiser, P. Guillaume, J. C. Cerottini, P. Romero, and D. Valmori. 2002. Functional avidity of tumor antigen-specific CTL recognition directly correlates with the stability of MHC/peptide multimer binding to TCR. *J. Immunol.* 168:1167-1171.

16. Dutoit, V., P. Guillaume, J. C. Cerottini, P. Romero, and D. Valmori. 2002. Dissecting TCR-MHC/peptide complex interactions with A2/peptide multimers

incorporating tumor antigen peptide variants: crucial role of interaction kinetics on functional outcomes. *Eur. J. Immunol.* 32:3285-3293.

17. Malherbe, L., C. Hausl, L. Teyton, and M. G. McHeyzer-Williams. 2004. Clonal selection of helper T cells is determined by an affinity threshold with no further skewing of TCR binding properties. *Immunity* 21:669-679.
18. Snyder, J. T., M. A. Alexander-Miller, J. A. Berzofskyl, and I. M. Belyakov. 2003. Molecular mechanisms and biological significance of CTL avidity. *Curr. HIV Res.* 1:287-294.
19. Barbey, C., P. Baumgaertner, E. Devevre, V. Rubio-Godoy, L. Derre, G. Bricard, P. Guillaume, I. F. Luescher, D. Lienard, J. C. Cerottini, P. Romero, N. Rufer, and D. E. Speiser. 2007. IL-12 controls cytotoxicity of a novel subset of self-antigen-specific human CD28+ cytolytic T cells. *J. Immunol.* 178:3566-3574.
20. Li, Y., R. Moysey, P. E. Molloy, A. L. Vuidepot, T. Mahon, E. Baston, S. Dunn, N. Liddy, J. Jacob, B. K. Jakobsen, and J. M. Boulter. 2005. Directed evolution of human T-cell receptors with picomolar affinities by phage display. *Nat. Biotechnol.* 23:349-354.
21. Dunn, S. M., P. J. Rizkallah, E. Baston, T. Mahon, B. Cameron, R. Moysey, F. Gao, M. Sami, J. Boulter, Y. Li, and B. K. Jakobsen. 2006. Directed evolution of human T cell receptor CDR2 residues by phage display dramatically enhances affinity for cognate peptide-MHC without increasing apparent cross-reactivity. *Protein Sci.* 15:710-721.
22. Holler, P. D., A. R. Lim, B. K. Cho, L. A. Rund, and D. M. Kranz. 2001. CD8(-) T cell transfectants that express a high affinity T cell receptor exhibit enhanced peptide-dependent activation. *J. Exp. Med.* 194:1043-1052.

23. Chlewicki, L. K., P. D. Holler, B. C. Monti, M. R. Clutter, and D. M. Kranz. 2005. High-affinity, peptide-specific T cell receptors can be generated by mutations in CDR1, CDR2 or CDR3. *J. Mol. Biol.* 346:223-239.

24. Zhao, Y., A. D. Bennett, Z. Zheng, Q. J. Wang, P. F. Robbins, L. Y. Yu, Y. Li, P. E. Molloy, S. M. Dunn, B. K. Jakobsen, S. A. Rosenberg, and R. A. Morgan. 2007. High-affinity TCRs generated by phage display provide CD4+ T cells with the ability to recognize and kill tumor cell lines. *J. Immunol.* 179:5845-5854.

25. Robbins, P. F., Y. F. Li, M. El-Gamil, Y. Zhao, J. A. Wargo, Z. Zheng, H. Xu, R. A. Morgan, S. A. Feldman, L. A. Johnson, A. D. Bennett, S. M. Dunn, T. M. Mahon, B. K. Jakobsen, and S. A. Rosenberg. 2008. Single and dual amino acid substitutions in TCR CDRs can enhance antigen-specific T cell functions. *J. Immunol.* 180:6116-6131.

26. Varela-Rohena, A., P. E. Molloy, S. M. Dunn, Y. Li, M. M. Suhoski, R. G. Carroll, A. Milicic, T. Mahon, D. H. Sutton, B. Laugel, R. Moysey, B. J. Cameron, A. Vuidepot, M. A. Purbhoo, D. K. Cole, R. E. Phillips, C. H. June, B. K. Jakobsen, A. K. Sewell, and J. L. Riley. 2008. Control of HIV-1 immune escape by CD8 T cells expressing enhanced T-cell receptor. *Nat. Med.* 14:1390-1395.

27. Holler, P. D., L. K. Chlewicki, and D. M. Kranz. 2003. TCRs with high affinity for foreign pMHC show self-reactivity. *Nat. Immunol.* 4:55-62.

28. Zoete, V., and O. Michielin. 2007. Comparison between computational alanine scanning and per-residue binding free energy decomposition for protein-protein association using MM-GBSA: application to the TCR-p-MHC complex. *Proteins* 67:1026-1047.

29. Zoete, V., M. B. Irving, and O. Michielin. 2010. MM-GBSA binding free energy decomposition and T cell receptor engineering. *J. Mol. Recognit.* 23:142-152.

30. Arden, B., S. P. Clark, D. Kabelitz, and T. W. Mak. 1995. Human T-cell receptor variable gene segment families. *Immunogenetics* 42:455-500.

31. Derre, L., M. Bruyninx, P. Baumgaertner, M. Ferber, D. Schmid, A. Leimgruber, V. Zoete, P. Romero, O. Michielin, D. E. Speiser, and N. Rufer. 2008. Distinct sets of alphabeta TCRs confer similar recognition of tumor antigen NY-ESO-1157-165 by interacting with its central Met/Trp residues. *Proc. Natl. Acad. Sci. USA* 105:15010-15015.

32. Dull, T., R. Zufferey, M. Kelly, R. J. Mandel, M. Nguyen, D. Trono, and L. Naldini. 1998. A third-generation lentivirus vector with a conditional packaging system. *J. Virol.* 72:8463-8471.

33. Derre, L., M. Bruyninx, P. Baumgaertner, E. Devevre, P. Corthesy, C. Touvrey, Y. D. Mahnke, H. Pircher, V. Voelter, P. Romero, D. E. Speiser, and N. Rufer. 2007. In Vivo Persistence of Codominant Human CD8+ T Cell Clonotypes Is Not Limited by Replicative Senescence or Functional Alteration. *J. Immunol.* 179:2368-2379.

34. Romero, P., V. Dutoit, V. Rubio-Godoy, D. Lienard, D. Speiser, P. Guillaume, K. Servis, D. Rimoldi, J. C. Cerottini, and D. Valmori. 2001. CD8+ T-cell response to NY-ESO-1: relative antigenicity and in vitro immunogenicity of natural and analogue sequences. *Clin. Cancer Res.* 7:766s-772s.

35. Le Gal, F. A., M. Ayyoub, V. Dutoit, V. Widmer, E. Jager, J. C. Cerottini, P. Y. Dietrich, and D. Valmori. 2005. Distinct structural TCR repertoires in naturally occurring versus vaccine-induced CD8+ T-cell responses to the tumor-specific antigen NY-ESO-1. *J. Immunother.* 28:252-257.

36. Chen, J. L., G. Stewart-Jones, G. Bossi, N. M. Lissin, L. Wooldridge, E. M. Choi, G. Held, P. R. Dunbar, R. M. Esnouf, M. Sami, J. M. Boulter, P. Rizkallah, C. Renner, A. Sewell, P. A. van der Merwe, B. K. Jakobsen, G. Griffiths, E. Y. Jones, and V. Cerundolo. 2005. Structural and kinetic basis for heightened immunogenicity of T cell vaccines. *J. Exp. Med.* 201:1243-1255.

37. Smith, S. D., R. Morgan, R. Gemmell, M. D. Amylon, M. P. Link, C. Linker, B. K. Hecht, R. Warnke, B. E. Glader, and F. Hecht. 1988. Clinical and biologic characterization of T-cell neoplasias with rearrangements of chromosome 7 band q34. *Blood* 71:395-402.

38. Boniface, J. J., J. D. Rabinowitz, C. Wulfing, J. Hampl, Z. Reich, J. D. Altman, R. M. Kantor, C. Beeson, H. M. McConnell, and M. M. Davis. 1998. Initiation of signal transduction through the T cell receptor requires the multivalent engagement of peptide/MHC ligands [corrected]. *Immunity* 9:459-466.

39. Minguet, S., M. Swamy, B. Alarcon, I. F. Luescher, and W. W. Schamel. 2007. Full activation of the T cell receptor requires both clustering and conformational changes at CD3. *Immunity* 26:43-54.

40. Berg, N. N., L. G. Puente, W. Dawicki, and H. L. Ostergaard. 1998. Sustained TCR signaling is required for mitogen-activated protein kinase activation and degranulation by cytotoxic T lymphocytes. *J. Immunol.* 161:2919-2924.

41. Ohnishi, H., K. Takeda, J. Domenico, J. J. Lucas, N. Miyahara, C. H. Swasey, A. Dakhama, and E. W. Gelfand. 2009. Mitogen-activated protein kinase/extracellular signal-regulated kinase 1/2-dependent pathways are essential for CD8+ T cell-mediated airway hyperresponsiveness and inflammation. *J. Allergy Clin. Immunol.* 123:249-257.

42. Pittet, M. J., V. Rubio-Godoy, G. Bioley, P. Guillaume, P. Batard, D. Speiser, I. Luescher, J. C. Cerottini, P. Romero, and A. Zippelius. 2003. Alpha 3 domain mutants of peptide/MHC class I multimers allow the selective isolation of high avidity tumor-reactive CD8 T cells. *J. Immunol.* 171:1844-1849.
43. Bendle, G. M., J. B. Haanen, and T. N. Schumacher. 2009. Preclinical development of T cell receptor gene therapy. *Curr. Opin. Immunol.* 21:209-214.
44. Rosenberg, S. A., and M. E. Dudley. 2009. Adoptive cell therapy for the treatment of patients with metastatic melanoma. *Curr. Opin. Immunol.* 21:233-240.
45. Morgan, R. A., M. E. Dudley, J. R. Wunderlich, M. S. Hughes, J. C. Yang, R. M. Sherry, R. E. Royal, S. L. Topalian, U. S. Kammula, N. P. Restifo, Z. Zheng, A. Nahvi, C. R. de Vries, L. J. Rogers-Freezer, S. A. Mavroukakis, and S. A. Rosenberg. 2006. Cancer regression in patients after transfer of genetically engineered lymphocytes. *Science* 314:126-129.
46. Johnson, L. A., R. A. Morgan, M. E. Dudley, L. Cassard, J. C. Yang, M. S. Hughes, U. S. Kammula, R. E. Royal, R. M. Sherry, J. R. Wunderlich, C. C. Lee, N. P. Restifo, S. L. Schwarz, A. P. Cogdill, R. J. Bishop, H. Kim, C. C. Brewer, S. F. Rudy, C. VanWaes, J. L. Davis, A. Mathur, R. T. Ripley, D. A. Nathan, C. M. Laurencot, and S. A. Rosenberg. 2009. Gene therapy with human and mouse T-cell receptors mediates cancer regression and targets normal tissues expressing cognate antigen. *Blood* 114:535-546.
47. Offringa, R. 2009. Antigen choice in adoptive T-cell therapy of cancer. *Curr. Opin. Immunol.* 21:190-199.
48. Krogsgaard, M., and M. M. Davis. 2005. How T cells 'see' antigen. *Nat. Immunol.* 6:239-245.

49. McKeithan, T. W. 1995. Kinetic proofreading in T-cell receptor signal transduction. *Proc. Natl. Acad. Sci. USA* 92:5042-5046.
50. Rabinowitz, J. D., C. Beeson, D. S. Lyons, M. M. Davis, and H. M. McConnell. 1996. Kinetic discrimination in T-cell activation. *Proc. Natl. Acad. Sci. USA* 93:1401-1405.
51. Valitutti, S., S. Muller, M. Cella, E. Padovan, and A. Lanzavecchia. 1995. Serial triggering of many T-cell receptors by a few peptide-MHC complexes. *Nature* 375:148-151.
52. Kalergis, A. M., N. Boucheron, M. A. Doucey, E. Palmieri, E. C. Goyarts, Z. Vegh, I. F. Luescher, and S. G. Nathenson. 2001. Efficient T cell activation requires an optimal dwell-time of interaction between the TCR and the pMHC complex. *Nat. Immunol.* 2:229-234.
53. Chervin, A. S., J. D. Stone, P. D. Holler, A. Bai, J. Chen, H. N. Eisen, and D. M. Kranz. 2009. The impact of TCR-binding properties and antigen presentation format on T cell responsiveness. *J. Immunol.* 183:1166-1178.

FIGURE LEGENDS

Figure 1. TCR-pMHC binding kinetics in primary CD8 T cells transduced with WT and variant TCRs. (A) TCR surface expression and specificity was evaluated in transduced bulk CD8 T cells by flow cytometry analysis using anti-BV13 Ab and A2/NY-ESO-$1_{157-165}$ multimers. Controls stainings with A2/CMVpp65 are depicted. Stainings of cells transduced with TCR 1G4 and wtc51 gave similar results (data not shown). To allow direct comparison between samples, we always used CD8 T cells expressing > 90% of transduced TCR BV13. Of note, the flow cytometry profiles represent a compiled set of data obtained from different experiments, accounting for some inter-experimental variations in terms of mean fluorescence intensity. The surface expression of each TCR variant was quantified in subsequent experiments described in Figure 1B to Figure 6. **(B)** The rate of association of multimers on transduced CD8 T cells was measured as described in *Materials and Methods*. **(C)** After staining transduced CD8 T cells with multimers, decay of staining was measured by flow cytometry over time. The percentage of initial bound multimer that remained associated with the cells after various time points is depicted as a representative experiment, and time for half maximal binding ($t_{1/2}$) was determined. **(D)** Average k_{off} values (dissociation constant of the pMHC from the TCR, min^{-1}) assessed during multimer dissociation assays and representative of eight independent experiments. Data were analyzed by unpaired two-sample *t* test. The dotted line was arbitrarily set at the k_{off} value obtained for WT TCR and allows direct comparison between the different transduced CD8 T cells. We also included the natural T cell clone (TCC) from which the WT TCR BV13-clono1 had been originally isolated. **(E)** Relationships between multimer off-rates (k_{off}, min^{-1}) and monomeric affinity (K_D,

μM) or off-rates (k_{off}, s^{-1}) as measured by SPR, expressed as log-log fitting straight lines.

Figure 2. Immuno-fluorescence stainings of SUP-T1 cells expressing WT TCR or V49I or G50A+A51E TCR variants. (A) Cells were incubated with PE-conjugated HLA-A2/NY-ESO-1 multimers before fixation and analyzed by confocal microscopy. **(B)** After acquisition, the raw images were deconvolved, processed and quantified as detailed in *Materials and Methods*. All data are representative of three independent experiments. Single cells expressing WT or V49I or G50A+A51E TCRs are depicted.

Figure 3. Levels of LAT and ERK phosphorylation in SUP-T1 and CD8 T cells expressing TCR variants. (A) TCR-untransduced (Ø) or TCR-transduced (WT, G50A+A51E, V49I) SUP-T1 or CD8 T cells were stimulated for 10 min at 37° C with A2/NY-ESO-$1_{157\text{-}165}$ multimer or with OKT3 in the presence of anti-CD28 mAb. All data are representative of at least three independent experiments. **(B)** CD8 T cells transduced with WT TCR or G50A+A51E variant were left unstimulated (t = 0) or were stimulated at 37°C for 1, 5, 10, 15 and 20 min with A2/NY-ESO-$1_{157\text{-}165}$ multimers in the presence of anti-CD28 mAb. Data are representative of four independent experiments. **(C)** To allow direct comparison between the different time-points, intensity of LAT and ERK2 phosphorylation levels relative to unstimulated samples (“unst” t0, arbitrarily set as 1) were quantified and subsequently normalized to β-actin. Inserts show the phosphorylation baseline of unstimulated cells (WT versus G50A+A51E) as assessed by anti-phosphotyrosine stainings. Mean values ± SEM are shown in each graph. **(A-C)** Cell lysates were assayed for levels of LAT (P-

Tyr and Y171) and ERK 1/2 phosphorylation. β-actin was used as a loading control to compare protein levels between samples. All transduced T cells expressed comparable proportions of transduced TCR BV13. **(D)** Relative proliferative capacity of CD8 T cells transduced with TCR variants normalized to the proliferative capacity of WT transduced T cells (represented by the dotted line). CFSE-labeled transduced CD8 T cells were assessed by flow cytometry at days 3 or 4 after stimulation with T2 cells pulsed with 0.01 μg/ml of NY-ESO-$1_{157\text{-}165}$ peptide as described in the *Materials and Methods*. Data from nine independent experiments are depicted.

Figure 4. Efficiency of NY-ESO-1 antigen recognition by CD8 T cells transduced with TCR variants. (A) The relative TCR avidity of each variant (filled symbols) was compared to WT transduced T cells (opened squares) using T2 target cells (HLA-$A2^{+}$/$TAP^{-/-}$) loaded with graded concentrations of analog (SLLMWITQA) NY-ESO-$1_{157\text{-}165}$ peptide. For each experiment, we included T2 cells pulsed with the irrelevant Melan-$A_{26\text{-}35}$ peptide (data not shown). **(B)** Complete collection of data (n = 16 independent experiments) representing the peptide concentration (in nM, log scale) used to achieve 50% of maximal lysis. WT TCR and TCR variants are classified according to their progressive increased affinities (by SPR). Each data point represents the result of an individual transduced CD8 T cells. Statistically significant p values are shown (unpaired two-sample *t* test). Of note, similar data were obtained when transduced T cells were tested against T2 cells pulsed with the native (SLLMWITQC) NY-ESO-$1_{157\text{-}165}$ peptide (data not shown).

Figure 5. Functional avidity analysis of primary CD8 T cells transduced with TCR variants. (A) Relationships between functional avidity (EC50, 50% maximal

target cell lysis, nM) and TCR-pMHC binding avidity (multimer off-rates) or affinity (SPR analysis). Functional avidities of CD8 transduced TCR variants are plotted against (i) multimer off-rates (k_{off}, min^{-1}) and (ii) monomeric affinity (K_D, μM). The dotted lines represent an arbitrarily set boundary separating two distinct groups of TCR variants. **(B)** Peptide recognition was assessed using cell line C1R expressing either wild-type (opened squares) or mutant CD8-null (filled diamonds) HLA-A2 molecules as target cells at a lymphocyte to target ratio of 10:1 in the presence of serial dilutions of the analog NY-ESO-$1_{157\text{-}165}$ peptide. Ag-specific lytic activity was assessed in a functional 4-h chromium release assay. Data were obtained from four independent experiments and fitting with log sigmoid curves (Prism). Averages of 50% maximal target cell lysis (in M) are depicted. n.a., not applicable.

Figure 6. Melanoma cell killing by CD8 T cells transduced with TCR variants. (A, B) Tumor reactivity for the melanoma cell lines Me 275 and Me 290 ($A2^+$/NY-ESO-1^+), and NA8-MEL ($A2^+$/NY-ESO-1^-) in the absence (A) or presence (B) of analog NY-ESO-$1_{157\text{-}165}$ peptide (1 μM) at the indicated target to effector ratio. Dotted lines are set at 50% of specific lysis to allow direct comparison between transduced CD8 T cell variants. **(C)** Killing ratio was estimated from the percentage of specific lysis obtained without adding exogenous peptide (A) versus the proportion of lysis obtained after adding exogenous peptide (B) at a target to effector ratio of 10:1. WT TCR and TCR variants are classified according to their progressive increased affinities (by SPR). Dotted lines are arbitrarily set at the average killing ratio values obtained for WT T cells, and allow direct comparison between the different CD8 T cell variants. Data are representative of twelve independent experiments. (D) Model integrating the relationship between functional avidity

(EC50, nM) and monomeric TCR affinity (K_D, μM) of CD8 transduced TCR WT and variants.

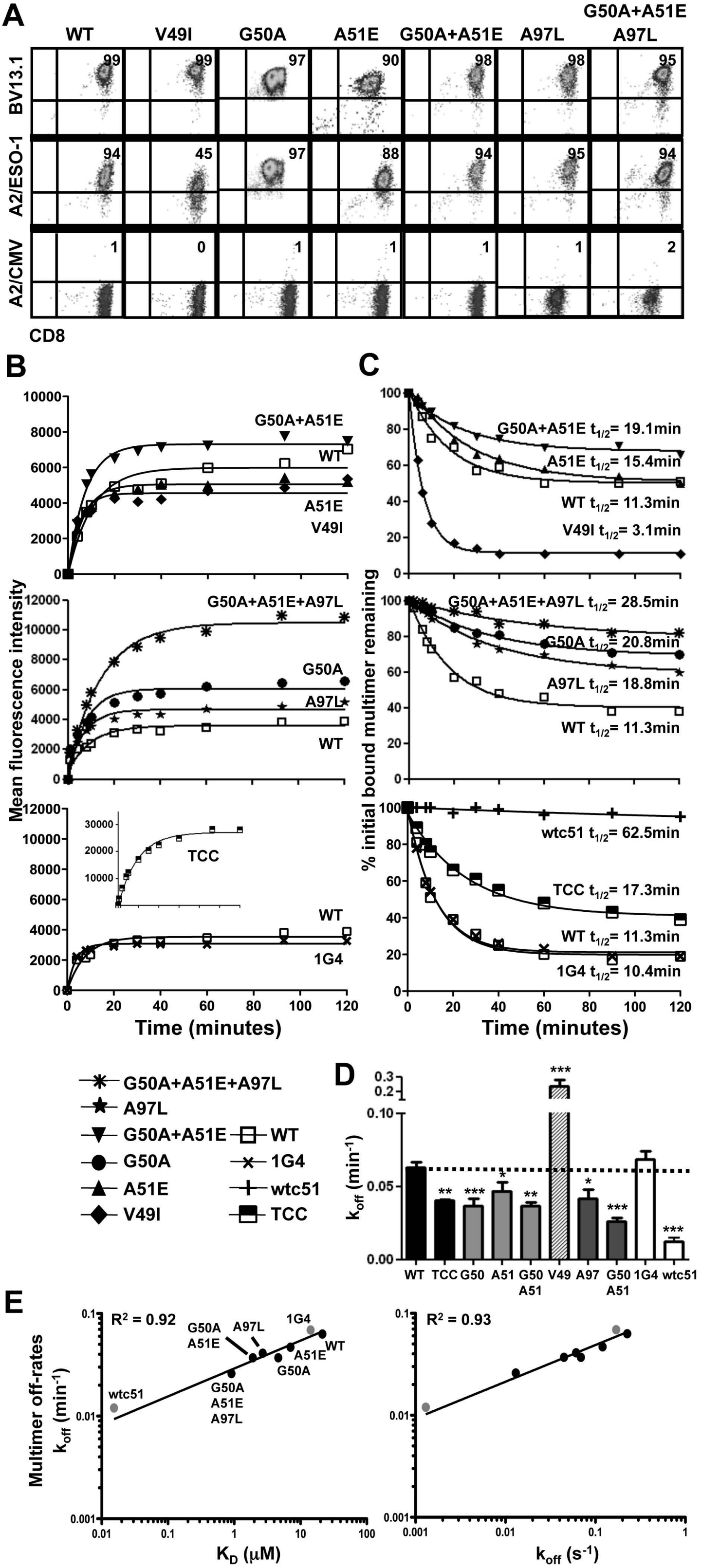
A
WT
V49I
G50A
A51E
G50A+A51E
A97L
G50A+A51E A97L
BV13.1
99
99
97
90
98
98
95
A2/ESO-1
94
45
97
88
94
95
94
A2/CMV
1
0
1
1
1
1
2
CD8
B
Mean fluorescence intensity
G50A+A51E
WT
A51E
V49I
G50A+A51E+A97L
G50A
A97L
WT
TCC
WT
1G4
Time (minutes)
C
% initial bound multimer remaining
G50A+A51E t1/2= 19.1min
A51E t1/2= 15.4min
WT t1/2= 11.3min
V49I t1/2= 3.1min
G50A+A51E+A97L t1/2= 28.5min
G50A t1/2= 20.8min
A97L t1/2= 18.8min
WT t1/2= 11.3min
wtc51 t1/2= 62.5min
TCC t1/2= 17.3min
WT t1/2= 11.3min
1G4 t1/2= 10.4min
Time (minutes)
G50A+A51E+A97L
A97L
G50A+A51E
WT
G50A
1G4
A51E
wtc51
V49I
TCC
D
koff (min-1)
***
**
***
*
**
*
***
***
WT
TCC
G50
A51
G50 A51
V49
A97
G50 A51
1G4
wtc51
E
Multimer off-rates koff (min-1)
R2 = 0.92
G50A A51E
A97L
1G4
WT
A51E
G50A
wtc51
G50A A51E A97L
KD (μM)
R2 = 0.93
koff (s-1)

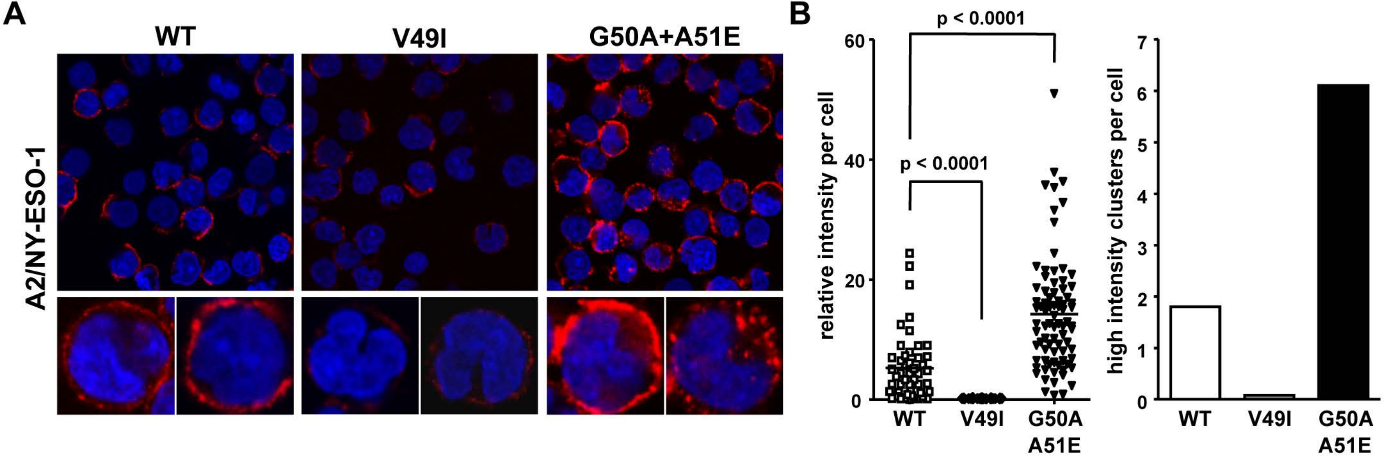
A
WT
V49I
G50A+A51E
A2/NY-ESO-1
B
p < 0.0001
p < 0.0001
60
40
20
0
relative intensity per cell
WT
V49I
G50A
A51E
7
6
5
4
3
2
1
0
high intensity clusters per cell
WT
V49I
G50A
A51E

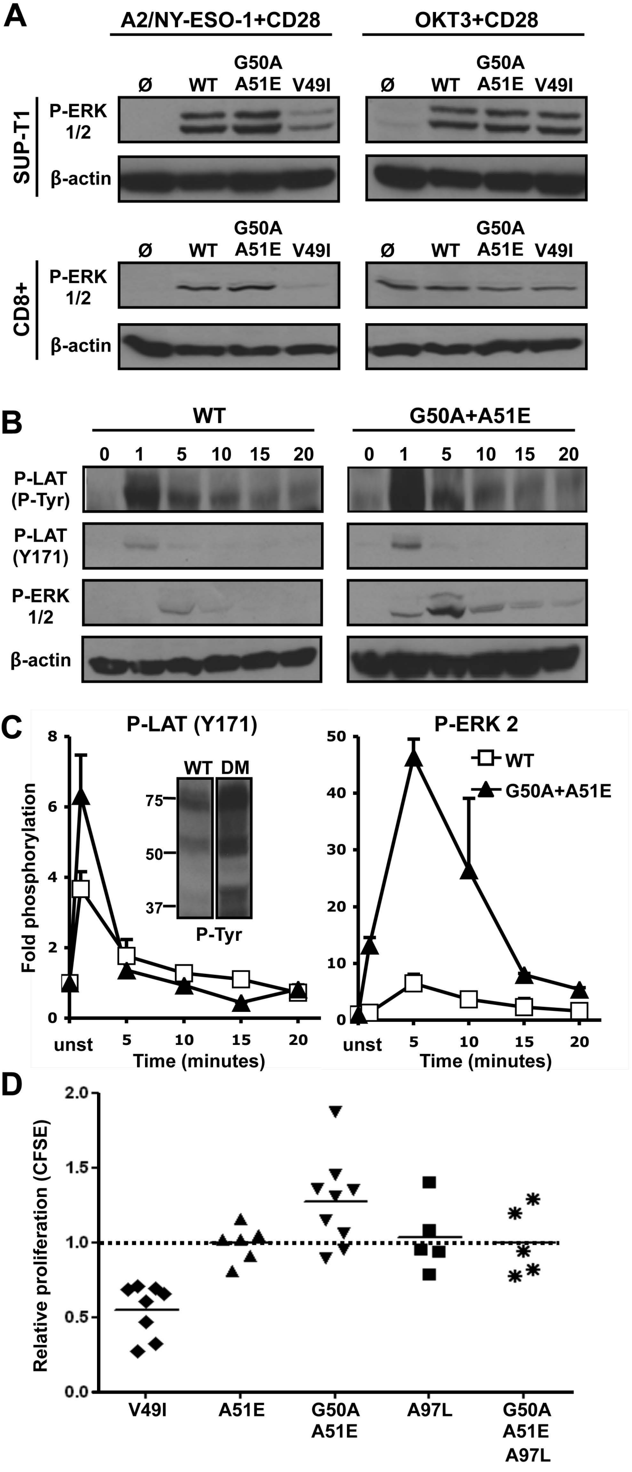
A
A2/NY-ESO-1+CD28
OKT3+CD28
Ø
WT
G50A A51E
V49I
SUP-T1
P-ERK 1/2
β-actin
CD8+
P-ERK 1/2
β-actin
B
WT
G50A+A51E
0 1 5 10 15 20
P-LAT (P-Tyr)
P-LAT (Y171)
P-ERK 1/2
β-actin
C
P-LAT (Y171)
Fold phosphorylation
WT DM
75
50
37
P-Tyr
0 2 4 6 8
unst 5 10 15 20
Time (minutes)
P-ERK 2
WT
G50A+A51E
0 10 20 30 40 50
unst 5 10 15 20
Time (minutes)
D
Relative proliferation (CFSE)
0.0 0.5 1.0 1.5 2.0
V49I
A51E
G50A A51E
A97L
G50A A51E A97L

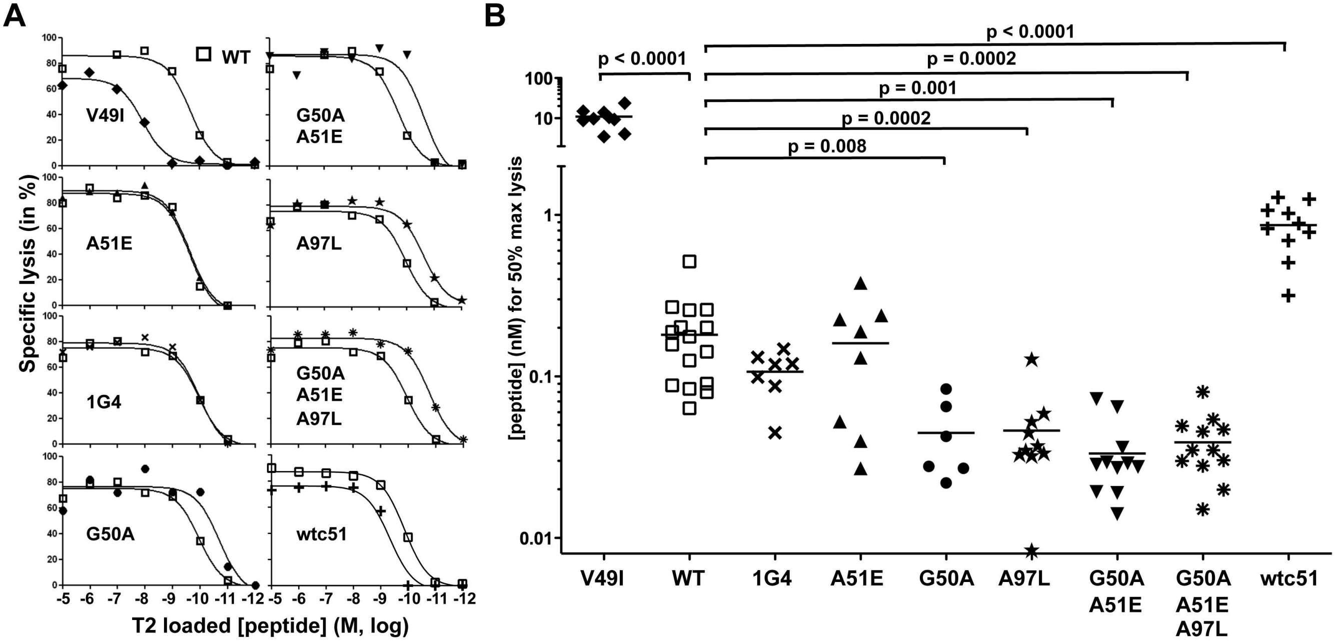
A
B
WT
V49I
G50A
A51E
A51E
A97L
1G4
G50A
A51E
A97L
G50A
wtc51
Specific lysis (in %)
0
20
40
60
80
100
-5
-6
-7
-8
-9
-10
-11
-12
T2 loaded [peptide] (M, log)
p < 0.0001
p < 0.0001
p = 0.0002
p = 0.001
p = 0.0002
p = 0.008
100
10
1
0.1
0.01
[peptide] (nM) for 50% max lysis
V49I
WT
1G4
A51E
G50A
A97L
G50A
A51E
G50A
A51E
A97L
wtc51

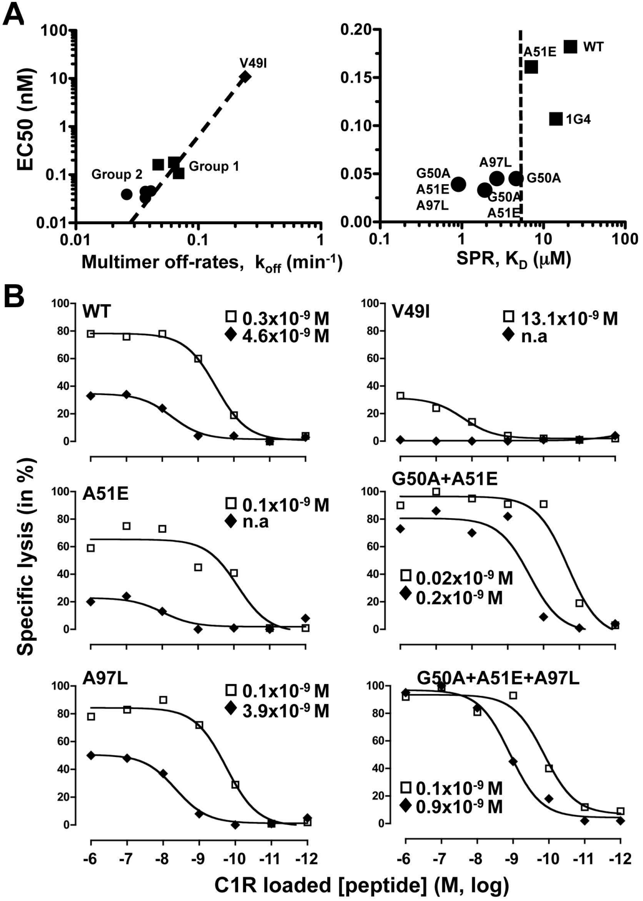
A
EC50 (nM)
100
10
1
0.1
0.01
V49I
Group 2
Group 1
0.01
0.1
1
Multimer off-rates, k_{off} (min^{-1})
0.20
0.15
0.10
0.05
0.00
A51E
WT
1G4
A97L
G50A
A51E
A97L
G50A
G50A
A51E
0.1
1
10
100
SPR, K_D (μM)
B
Specific lysis (in %)
WT
0.3x10^{-9} M
4.6x10^{-9} M
V49I
13.1x10^{-9} M
n.a
A51E
0.1x10^{-9} M
n.a
G50A+A51E
0.02x10^{-9} M
0.2x10^{-9} M
A97L
0.1x10^{-9} M
3.9x10^{-9} M
G50A+A51E+A97L
0.1x10^{-9} M
0.9x10^{-9} M
100
80
60
40
20
0
-6
-7
-8
-9
-10
-11
-12
C1R loaded [peptide] (M, log)

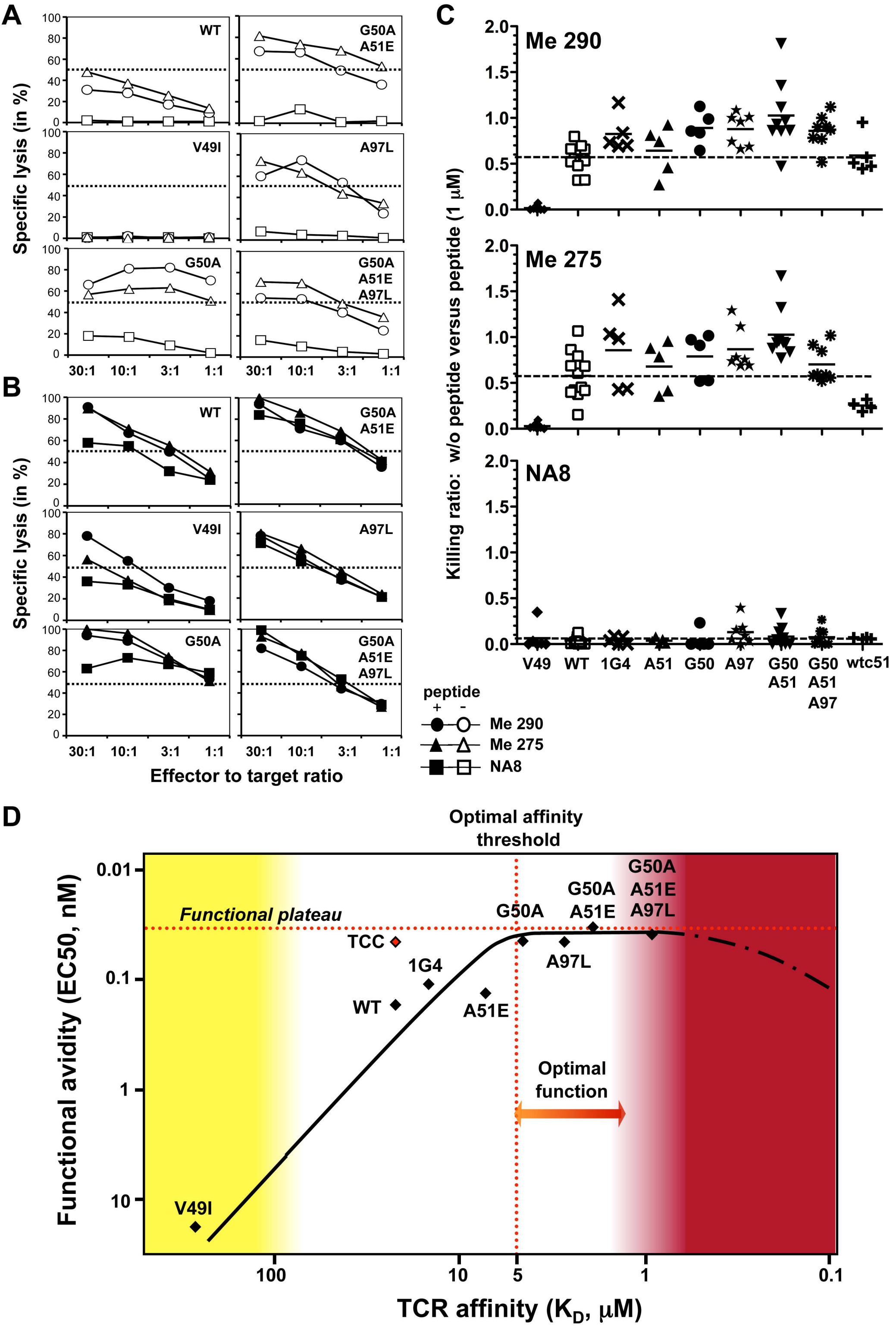
A
Specific lysis (in %)
WT
G50A A51E
V49I
A97L
G50A
G50A A51E A97L
100 80 60 40 20 0
30:1 10:1 3:1 1:1
B
Specific lysis (in %)
WT
G50A A51E
V49I
A97L
G50A
G50A A51E A97L
Effector to target ratio
peptide
+ -
Me 290
Me 275
NA8
C
Killing ratio: w/o peptide versus peptide (1 μM)
Me 290
Me 275
NA8
0.0 0.5 1.0 1.5 2.0
V49
WT
1G4
A51
G50
A97
G50 A51
G50 A51 A97
wtc51
D
Optimal affinity threshold
Functional plateau
Functional avidity (EC50, nM)
0.01
0.1
1
10
TCC
1G4
WT
A51E
G50A
G50A A51E
G50A A51E A97L
A97L
V49I
Optimal function
TCR affinity (K_D, μM)
100
10
5
1
0.1

ONLINE

Supplemental Figure1. TCR-pMHC binding kinetics in SUP-T1 cells transduced with WT and variant TCRs. (A) TCR surface expression and specificity was evaluated in transduced SUP-T1 cells by flow cytometry analysis using anti-BV13 Ab and A2/NY-ESO-$1_{157\text{-}165}$ multimers. Stainings of cells transduced with TCR 1G4 and wtc51 gave similar results (data not shown). To allow direct comparison between samples, we always used SUP-T1 cells expressing > 90% of transduced TCR BV13. **(B)** The rate of association of multimers on transduced SUP-T1 cells was measured as described in *Materials and Methods*. Background levels were assessed with SUP-T1 cells expressing an irrelevant Melan-A specific TCR. **(C)** After staining transduced SUP-T1 cells with multimers, decay of staining was measured by flow cytometry over time. The percentage of initial bound multimer that remained associated with the cells after various time points is depicted for a representative experiment and time for half maximal binding ($t_{1/2}$) was determined. **(D)** Average k_{off} values (dissociation constant of the pMHC from the TCR, min^{-1}) assessed during multimer dissociation assays and representative of nine independent experiments. Data were analyzed by unpaired two-sample *t* test. The dotted line was arbitrarily set at the k_{off} value obtained for WT TCR and allows direct comparison between the different transduced SUP-T1 cells. **(E)** Relationships between multimer off-rates (k_{off}, min^{-1}) and monomeric affinity (K_D, μM) or off-rates (k_{off}, s^{-1}) as measured by SPR, expressed as log-log fitting straight lines.

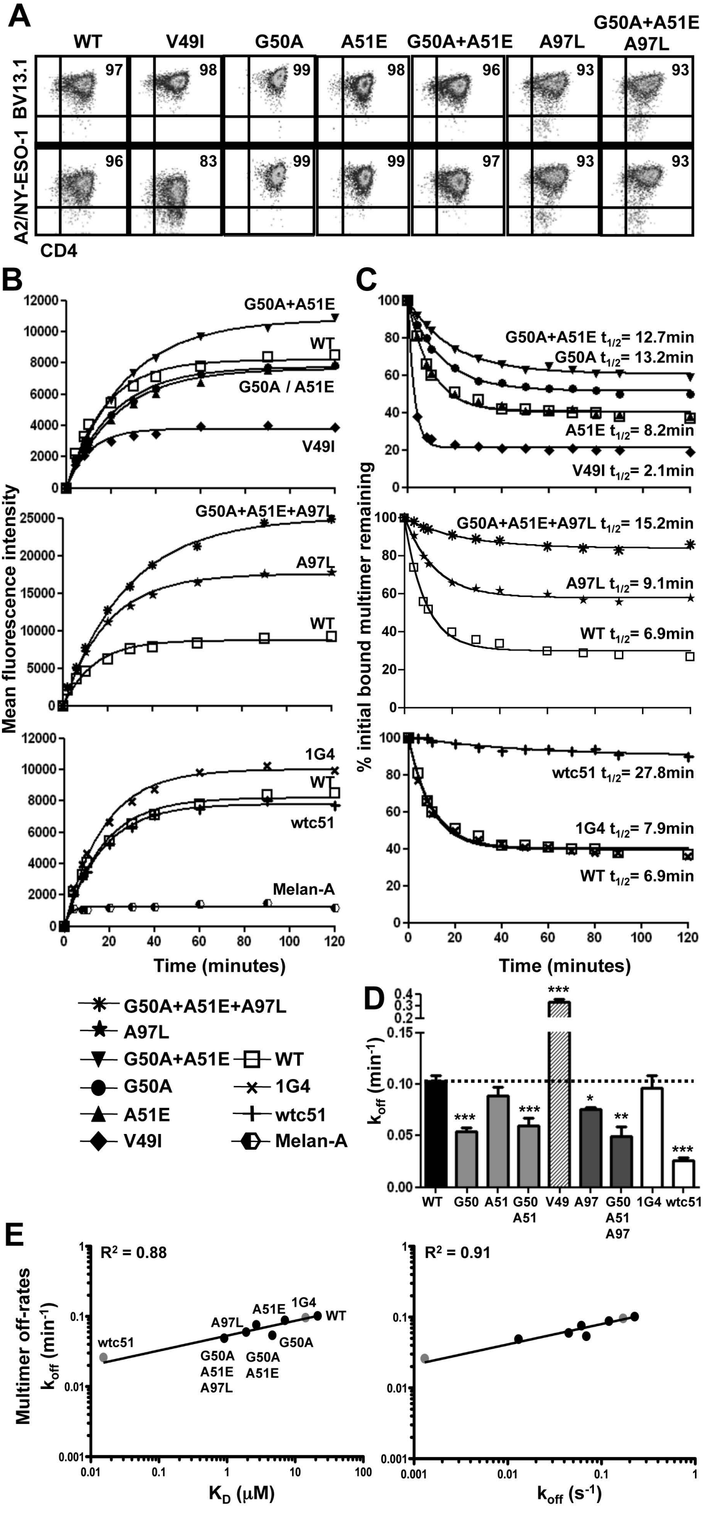
A
WT
V49I
G50A
A51E
G50A+A51E
A97L
G50A+A51E
A97L
BV13.1
A2/NY-ESO-1
CD4
97
98
99
98
96
93
93
96
83
99
99
97
93
93
B
Mean fluorescence intensity
G50A+A51E
WT
G50A / A51E
V49I
G50A+A51E+A97L
A97L
WT
1G4
WT
wtc51
Melan-A
Time (minutes)
C
% initial bound multimer remaining
G50A+A51E $t_{1/2}$= 12.7min
G50A $t_{1/2}$= 13.2min
A51E $t_{1/2}$= 8.2min
V49I $t_{1/2}$= 2.1min
G50A+A51E+A97L $t_{1/2}$= 15.2min
A97L $t_{1/2}$= 9.1min
WT $t_{1/2}$= 6.9min
wtc51 $t_{1/2}$= 27.8min
1G4 $t_{1/2}$= 7.9min
WT $t_{1/2}$= 6.9min
Time (minutes)
G50A+A51E+A97L
A97L
G50A+A51E
WT
G50A
1G4
A51E
wtc51
V49I
Melan-A
D
k_{off} (min^{-1})
***
***
***
*
**
***
***
WT
G50
A51
G50 A51
V49
A97
G50 A51 A97
1G4
wtc51
E
Multimer off-rates k_{off} (min^{-1})
R^2 = 0.88
wtc51
A97L
A51E
1G4
WT
G50A
G50A A51E A97L
G50A A51E
K_D (μM)
R^2 = 0.91
k_{off} (s^{-1})